Corrosion of Newly Manufactured Nanocrystalline Al and Two of its Alloys in stagnant 4.0% NaCl Solutions

El-Sayed M. Sherif [1,2,*], Hany S. Abdo [1,3], Jabair A. Mohammed [1], Abdulhakim A. Almajid [1,4] and Asiful H. Seikh [1]

[1]Center of Excellence for Research in Engineering Materials (CEREM), Advanced Manufacturing Institute, King Saud University, P. O. Box 800, Al-Riyadh 11421, Saudi Arabia
[2]Electrochemistry and Corrosion Laboratory, Department of Physical Chemistry, National Research Centre (NRC), Dokki, 12622 Cairo, Egypt
[3]Mechanical Design and Materials Department, Faculty of Energy Engineering, Aswan University, Aswan 81521, Egypt
[4] Mechanical Engineering Department, King Saud University, P.D. Box 800, Riyadh 11421, Saudi Arabia
[*]E-mail: esherif@ksu.edu.sa, emsherif@gmail.com

In this study, pure nanocrystalline Al and two of its alloys; namely Al-7%Cu and Al-7%Cu-3%Ti, were manufactured after 5.0 h milling period of time using mechanical attrition. All samples were sintered for 3 min at 600 °C using high frequency heat induction sintering furnace. The sizes of the crystallite and the hardness of the manufactured Al and its alloys were determined using X-ray diffractometer and Vickers hardness (VH) investigations, respectively. The effect of adding 7%Cu and 7%Cu+3%Ti on the corrosion of the fabricated pure aluminum in 4.0% NaCl solutions was carried out. The corrosion tests used in this study were cyclic polarization, change of current with time, and electrochemical impedance spectroscopy measurements. It was found that the presence of Cu increases the hardness of Al and this effect was highly increased in the presence of Cu and Ti together with Al. Moreover, adding Cu and further Cu and Ti increased the corrosion of Al. Adding Cu and Cu with Ti was found to increase the corrosion current, corrosion rate, anodic current, and cathodic current of Al. All results were consistent with each other and proved that the presence of Cu and Ti increases the hardness as well as the corrosion behavior of Al.

1. INTRODUCTION

Metal aluminum-based matrix composites have been considered as an outstanding substitute material because of its high corrosion resistance, excellent thermal conductivity, good mechanical properties, and acceptable ductility [1-8]. Developing new techniques for improving the physical and chemical properties of aluminum alloys has recently attracted a great attention [9]. Getting an increased mechanical properties can be obtained by using very fine particles (< 1μm) as reinforcement [10]. Decreasing the reinforcement particle size has been reported [11,12] to increase the mechanical strength. The high mechanical properties by the presence of reinforcement particles can be attributed to the elastic interactions between the particles and matrix dislocations. The type, size, morphology, volume fraction, and overall distribution affect the efficiency by which the reinforcement particles strengthen the metal- based matrix [13].

Aluminum and its alloys have many industrial applications for their thermal and electrical conductivities, easy to deform, light weight, high ductility and their resistance against corrosion [14-17]. Aluminum alloys have especial applications in regard to their reactivity and corrosion reactions, where they can be employed as anodes in alkaline batteries as well as sacrificial anodes to protect metallic structures in the cathodic protection systems. It is well known that aluminum and most of its alloys develop an oxide film on their surfaces upon exposing to air. This film is very immune and has higher corrosion resistance compared to the aluminum surface itself, which makes aluminum and its alloys are not well sacrificial anodes when connected to more noble metallic structure. One of the most employed techniques to activate the corrosion of aluminum is the use of alloying elements.

The influence of adding zinc, titanium, mercury, and indium on activation of aluminium to be used as sacrificial anode reported [18,19]. This was started many decades ago with Schreiber and Reding [20] who performed comprehensive tests on the activation of aluminum and come up with an A1/Zn/Hg anode, which maintains a relatively negative potential and an efficiency of 95%. Sakano et al. [21] have developed the Al/Zn/In alloy as sacrificial anode, which provides 90% efficiency. More recently, Shibli and Gireesh [22] studied the activation of Al+5%Zn alloy anode by iridium oxide surface coatings. Shibli et al. [23] also reported the effect of nano cerium and zinc oxides on the activation of Al-Zn matrix and found that the new aluminum anode gives a performance of 78.62% at an optimized nano cerium oxide content of 0.2%.

The current work reports the manufacturing of nanocrystalline metallic forms of pure Al, Al-7%Cu alloy and Al-7%Cu-3%Ti alloy. The aim was extended to report the hardness and corrosion resistance of these materials in 4.0% NaCl solutions. The fabrication procedures included the use of mechanical attrition for 5.0 h to refine the crystallite size and a high frequency heat induction sintering furnace (HFHISF) was employed for the materials' consolidation. The crystallite size was characterized using X-ray diffraction and the strength was measured using Vickers hardness. The corrosion behavior after immersion in 4.0% NaCl solution for 1.0 h and 24 h of all manufactured materials was performed using polarization, EIS, and change of current with time at -600 mV. The corroded surface of these materials analyzed using scanning electron microscope and energy dispersive X-ray analyzer. It was expected that the hardness of aluminum would significantly increase through the addition of Cu and Cu with Ti, while the corrosion resistance would decrease.

2. EXPERIMENTAL PART

2.1. Manufacturing of aluminum and its alloys

Pure aluminum (Al, 98%), copper (Cu, 99.99%), and titanium (Ti, 99.99%) powders (particle size ~ 100 micron) were obtained from Loba Chemie, India. The ball milling of Al, Cu and Ti powders was carried out in a 1S-attritor ball mill and results in producing a large quantity of heat inside the tank due to the strong collision among the balls and the powders. For the purpose of keeping the metal powders inside the tank of the attritor close to room temperature, running water was supplied through the jacket surrounding the tank for cooling the container and keeping the temperature inside the tank close to room temperature. All fabrication procedures were carried out as reported in our previous work [24] and the consolidation was performed after 5.0 h ball milling time.

2.2. XR and hardness measurements

The powders and milled aluminum as well as Al-7%Cu and Al-7%Cu-3%Ti milled for 5.0 h were investigated using BRUKER, D8_Discover X-ray diffractometer. Buehler 5100 series Micro Hardness Measuring Machine was employed to evaluate the Vickers hardness of the fabricated materials. The load was 100 gm/f and the dwell time was 10 seconds. The hardness measurement was repeated for 5 times and the average was taken to represent the hardness value.

2.3. Electrolyte, electrochemical cell, and electrochemical measurements

The electrolyte was 4.0% NaCl solution prepared from sodium chloride salt with 99% purity. A conventional electrochemical cell consists of three electrodes that accommodates for 300 cm^3 was employed in this study. The aluminum and its alloys were used as the working electrodes; an Ag/AgCl in 3 M KCl solution was used as the reference electrode; and a platinum sheet was employed as the counter electrode. The aluminum electrodes for electrochemical measurements were welded, mounted in epoxy, and ground as previously reported [24,25].

The electrochemical measurements were carried out using an Autolab Potentiostat-Galvanostat, which was made and purchased from the Netherlands. The polarization curves were obtained via scanning the potential from −1800 mV towards the positive direction to -400 mV at a scan rate of 1.0 mV/s (Ag/AgCl). The backward scan was performed directly from -400 mV at the same scan rate. Electrochemical impedance spectroscopy (EIS) data were obtained at an open circuit potential a change of frequency from 100 kHz to 1 mHz using an AC wave of ±5 mV peak-to-peak overlaid on a DC bias potential. Powersine software was used at a rate of 10 points per decade change in frequency to obtain the EIS data. The chronoamperometric current-time with change of time curves were obtained at -600 mV vs. Ag/AgCl after immersing the aluminum and its alloys in 4.0% NaCl solutions for 1.0 h and 24 h. All the measurements were obtained using a fresh surface of aluminum and aluminum alloys' electrodes and a new portion of 4.0% NaCl solution at room temperature.

2.4. SEM and EDX investigations

A scanning electron microscope with an energy dispersive X-ray analyzer attached were both obtained from JEOL (made in Tokyo, Japan) and were used to obtain the SEM images and EDX profiles for the surface of the aluminum and its alloys.

3. RESULTS AND DISCUSSION

3.1. XRD and hardness investigations

The XRD patterns obtained for the powders of (a) as received aluminum, (b) aluminum milled for 5.0 h, (c) Al-7%Cu milled for 5.0 h, and (d) Al-7%Cu-3%Ti milled for 5.0 h, respectively are shown in Figure 1. The XRD pattern obtained for the aluminum that was not treated (Figure 1a) depicts the narrowest peaks. On the other hand, these peaks get broaden after ball milling the aluminum for 5.0 h as can be seen from Figure 1b. The adding of copper and titanium and milling the mixtures for 5.0 h gives wider peaks, which proves that the grain size of the Al, Cu, and Ti get refined by being milled in the attritor (see Figure 1c and Figure 1d).
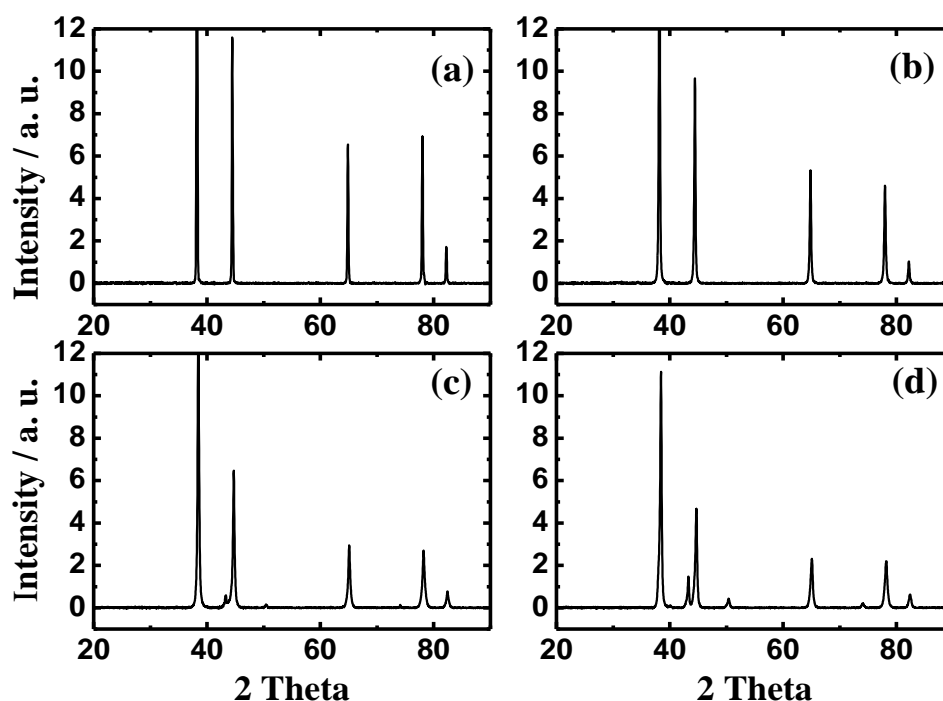

Figure 1. XRD patterns of the powders of (a) as received aluminum, (b) aluminum milled for 5.0 h, (c) Al-7%Cu milled for 5.0 h, and (d) Al-7%Cu-3%Ti milled for 5.0 h, respectively.

Figure 2 shows the average Vickers hardness obtained for pure nanocrystalline Al, Al-7%Cu alloy, and Al-7%Cu-3%Ti alloy after 5.0 h milling in the attritor ball mill under vacuum. The measurements of five runs were also listed in Table 1. It is clearly seen from Figure 2 and Table 1 that the Vickers hardness highly increased in the presence of Cu and further in the presence of Cu with Ti.

According to Rana et al. [26] and Shabestari and Moemeni [27], the addition of Cu to Al increases its hardness and improves its mechanical properties, which is due to the precipitation of copper bearing phase in the interdendritc space inside the aluminum. The current work thus aggress with the previous studies [25-28] that the addition of Cu increases the hardness and improves the mechanical properties of Al and that effect strongly increased when adding Cu with Ti together to Al.
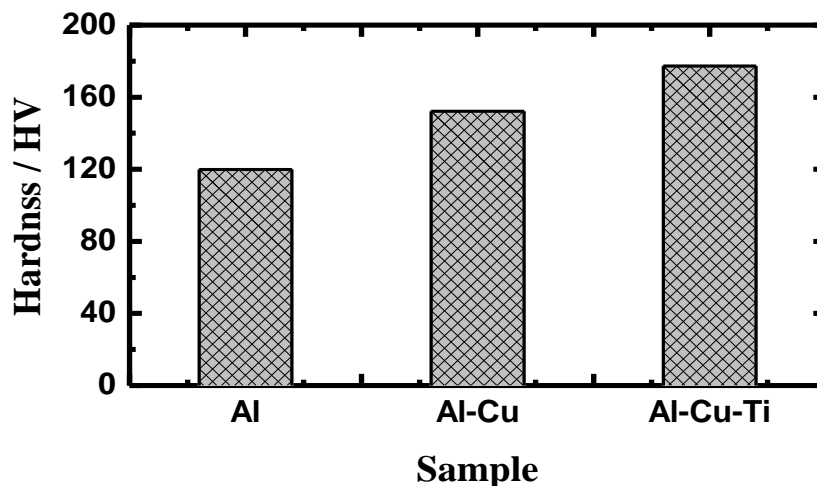

Figure 2. Average Vickers hardness obtained for pure Al, Al-7%Cu, and Al-7%Cu-3%Ti after 5 h milling in the attritor ball mill under vacuum.

Table 1. Change of Vickers hardness obtained for the pure nanocrystalline Al, Al-7%Cu, and Al-7%Cu-3%Ti after 5.0 h milling in the attritor ball mill under vacuum.

Reading number	Sample		
	Pure Al	**Al-7%Cu**	**Al-7%Cu-3%Ti**
1	124.1	151.2	88.1
2	119.2	149.5	86.7
3	118.4	152.5	85.8
4	122.0	159.9	87.8
5	115.5	147.8	89.4

3.2. Cyclic potentiodynamic polarization measurements

Figure 3 shows the cyclic potentiodynamic polarization (CPP) curves obtained for (1) pure Al, (2) Al-7%Cu, and (3) Al-7%Cu-3%Ti electrodes after their immersion for 1.0 h in 4% NaCl solutions, respectively. Similar measurements were obtained for the same materials after their immersion in 4.0% NaCl solutions for 24 h and the curves are shown in Figure 4. The values of the cathodic Tafel (β_c) and anodic Tafel (β_a) slopes, corrosion potential (E_{Corr}), corrosion current density (j_{Corr}) and polarization

resistance (R_p) that were obtained from the polarization curves shown in Figure 3 and Figure 4 are recorded Table 2. All these values were obtained as has been reported in our previous studies [28-30].
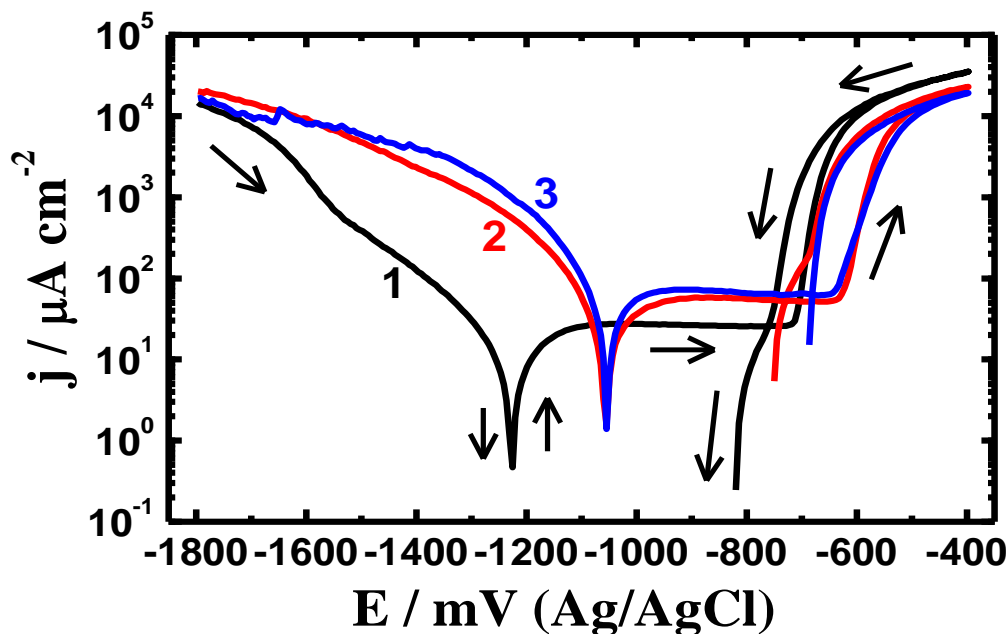

Figure 3. CPP curves of (1) pure Al, (2) Al-7%Cu, and (3) Al-7%Cu-3%Ti electrodes after their immersion for 1 h in 4% NaCl solutions, respectively.
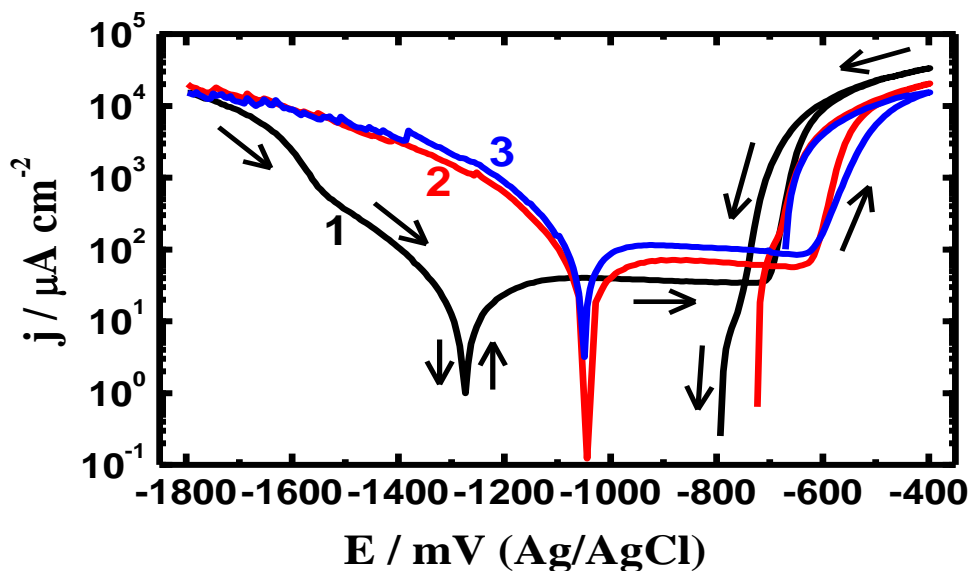

Figure 4. CPP curves of (1) pure Al, (2) Al-7%Cu, and (3) Al-7%Cu-3%Ti electrodes after their immersion for 24 h in 4% NaCl solutions, respectively.

It is seen from Figure 3 and Figure 4 as well as Table 2 that the presence of 7%Cu greatly increased the corrosion of Al. Furthermore, the addition of 3%Ti to the Al-7%Cu alloy highly increased the corrosion of Al and Al-Cu alloy both after 1 h and 24 h immersion in the chloride test

solution. This was confirmed by the increase of the corrosion parameters. Where, the value of j_{Corr} for Al immersed in NaCl solution for 1 h before measurement increased from 10μA/cm^2 to 28μA/cm^2 in the presence of 7%Cu and further to 42μA/cm^2 in the presence of 7%Cu+3%Ti. This is in addition to the increase of the anodic and cathodic currents, the less negative shift of E_{Corr} values as can be noted from Figure 3 and Figure 4. Also, the corrosion rate (R_{Corr}) increased in the presence of both Cu and Ti within Al. It is worth mentioning that the increase of immersion time from 1.0 h to 24 h increases the corrosion of all tested materials and this is due to the aggressiveness action of the chloride ions, which increases with the increase of time of exposure. This was confirmed by the data listed in Table 2, where the values of j_{Corr} and R_{Corr} increased when the time of exposure increased for Al, Al-Cu and Al-Cu-Ti alloys.

Table 2. Parameters obtained from the CPP curves for Al and its alloys in the 4.0% NaCl solutions.

Sample	Corrosion parameter					
	β_c / Vdec^{-1}	E_{Corr} / V	β_a / Vdec^{-1}	j_{Corr} / μA cm^{-2}	R_p / Ω cm^2	R_{Corr} / mpy
Pure Al (1 h)	0.155	−1.225	0.210	10.0	3877	0.1091
Al-7%Cu (1 h)	0.150	−1.030	0.225	28.0	1398	0.3587
Al-7%Cu-3%Ti (1 h)	0.140	−1.020	0.225	42.0	893	0.5563
Pure Al (24 h)	0.140	−1.270	0.190	12.0	2921	0.1309
Al-7%Cu (24 h)	0.130	−1.025	0.210	38.0	919	0.4868
Al-7%Cu-3%Ti (24 h)	0.120	−1.040	0.230	65.0	527	0.8610

3.3. Electrochemical impedance spectroscopy (EIS) measurements
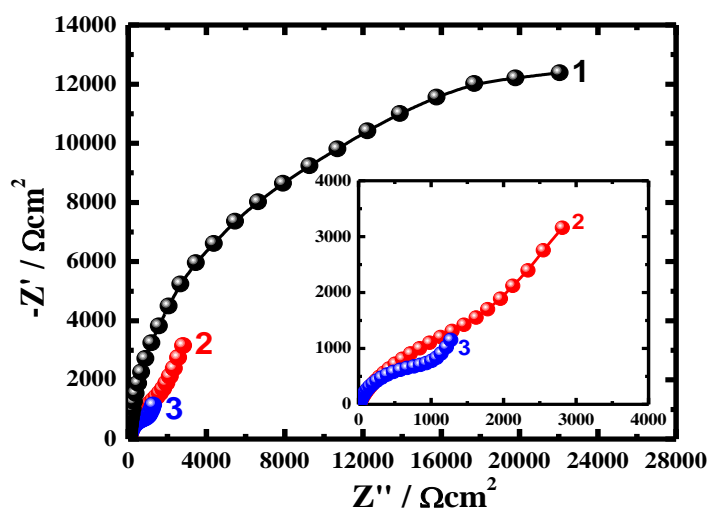

Figure 5. Nyquist plots of (1) pure Al, (2) Al-7%Cu, and (3) Al-7%Cu-3%Ti electrodes obtained after 1.0 h immersion in 4% NaCl solutions.

Typical Nyquist plots obtained after 1.0 h immersion in 4% NaCl solutions for (1) pure Al, (2) Al-7%Cu, and (3) Al-7%Cu-3%Ti electrodes, respectively are shown in Figure 5. The Nyquist plots obtained after 24 h for the same materials at the same conditions are also shown in Figure 6. The EIS experimental data were best fitted to the equivalent circuit model shown in Figure 7, which was also used to fit the impedance data obtained for the pure aluminum. The values of the impedance elements shown on the circuit of Figure 7 are listed in Table 3. It is well known that R_S is a solution resistance, Q is constant phase elements (CPEs), R_{P1} is a polarization resistance between the interface of electrode/solution chloride test solution, C_{dl} is a double layer capacitance at the interface of the, and R_{P2} is another polarization resistance between the surface product/solution interface.
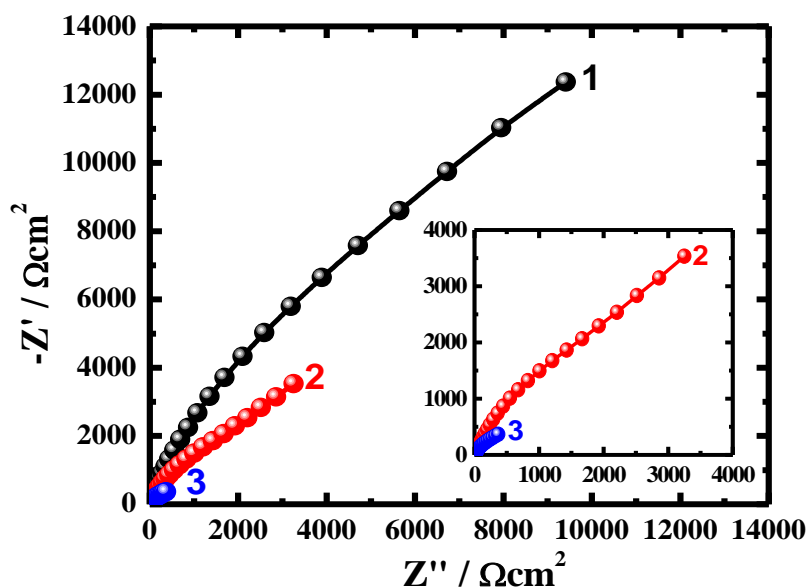

Figure 6. Nyquist plots of (1) pure Al, (2) Al-7%Cu, and (3) Al-7%Cu-3%Ti electrodes after 24 h immersion in 4% NaCl solutions.
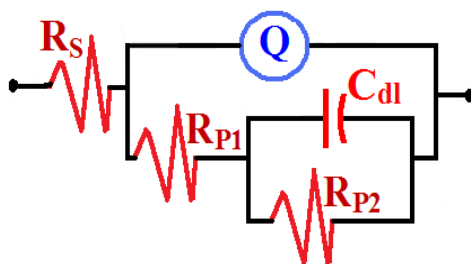

Figure 7. The equivalent circuit model used to fit EIS experimental data.

It is clearly seen from Figure 5 and Figure 6 that the diameter of the obtained semicircle decreased in the presence of Cu and further decreased in the presence of Cu with Ti, which indicates that the corrosion resistance of Al decreased by the addition of Cu and gets to the lowest by the presence of Cu and Ti with Al. This behavior was further confirmed by the values of the symbols listed in Table 3, where the presence of Cu decreased the values polarization resistances and increased the

values of the double layer capacitors both after 1.0 h and 24 h immersion in the chloride test solution. It is also seen that the increase of immersion time of the aluminum and its alloys to 24 h in the solution before measurements increased the corrosion via decreasing the diameter of the semicircle for all materials compared to its size after only 1.0 h immersion.

In order to give more evidences on the impedance behavior of the aluminum and its alloys, the change of (a) the Bode impedance of the interface and (b) the Bode phase angle with the change of frequency for (1) Al, (2) Al-7%Cu, and (3) Al-7%Cu-3%Ti electrodes after their immersion in 4.0 NaCl solutions for 1.0 h and 24 h were plotted as shown in Figure 8 and Figure 9, respectively. It is generally believed that the increase of |Z| values at low frequency regions means the resistance against corrosion is also increased. Furthermore, the increased the maximum value of phase angle at low frequency values provides more evidences on the increased corrosion resistance.

Table 3. EIS data obtained from the polarization curves for nanocrystalline Al and its alloys in the 4.0% NaCl solutions.

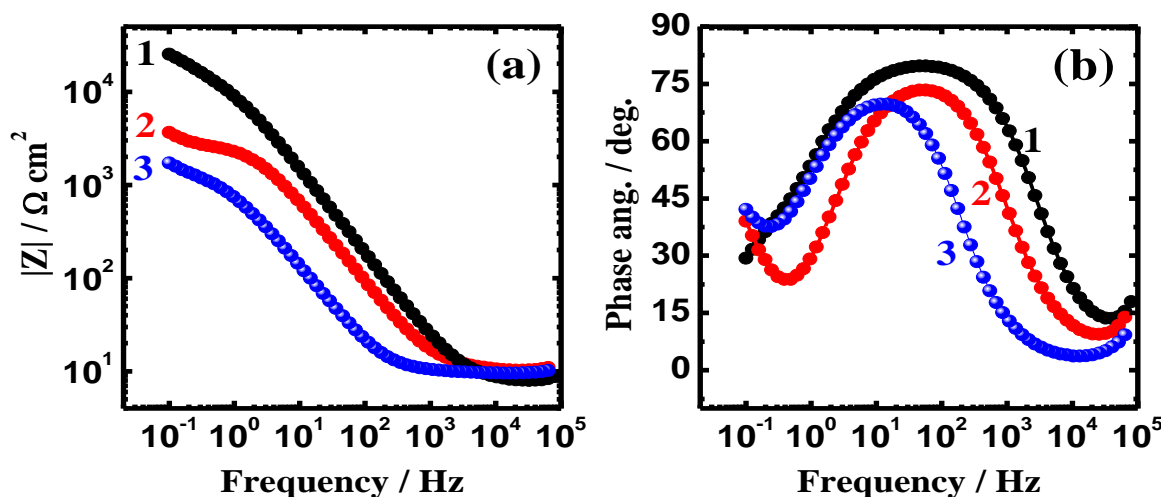| Sample	R_S / Ω cm^2	Q		R_{P1} / Ω cm^2	C_{dl} / F cm^{-2}	R_{P2} / Ω cm^2
		Y_{Q1}/ Fcm^{-2}	n			
Pure Al (1 h)	13.12	0.02044	0.80	2327	0.0652	4693
Al-7%Cu (1 h)	12.85	0.08774	0.80	1245	0.0979	2039
Al-7%Cu-3%Ti (1 h)	11.34	0.18520	0.89	819	0.1120	1453
Pure Al (24 h)	13.73	0.00638	0.74	2013	0.0942	3569
Al-7%Cu (24 h)	12.44	0.00859	0.64	525	0.1973	1363
Al-7%Cu-3%Ti (24 h)	11.74	0.008451	0.52	259	0.3036	686

Figure 8. Bode (a) impedance of the interface and (b) phase angle plots obtained after 1.0 h immersion in 4% NaCl solutions for (1) pure Al, (2) Al-7%Cu, and (3) Al-7%Cu-3%Ti.

Here, the highest values for |Z| at the low frequency regions and maximum value of Φ seen in Figure 8 and Figure 9 are recorded for Al followed by Al-7%Cu alloy and the lowest values were recorded for Al-7%Cu-3%Ti alloy. The EIS data (obtained by either Nyquist or Bode plots) are in good agreement with the measurements obtained by cyclic polarization technique that the corrosion of aluminum increases by the addition of 7%Cu and further increases with the presence of 7%Cu+3%Ti.
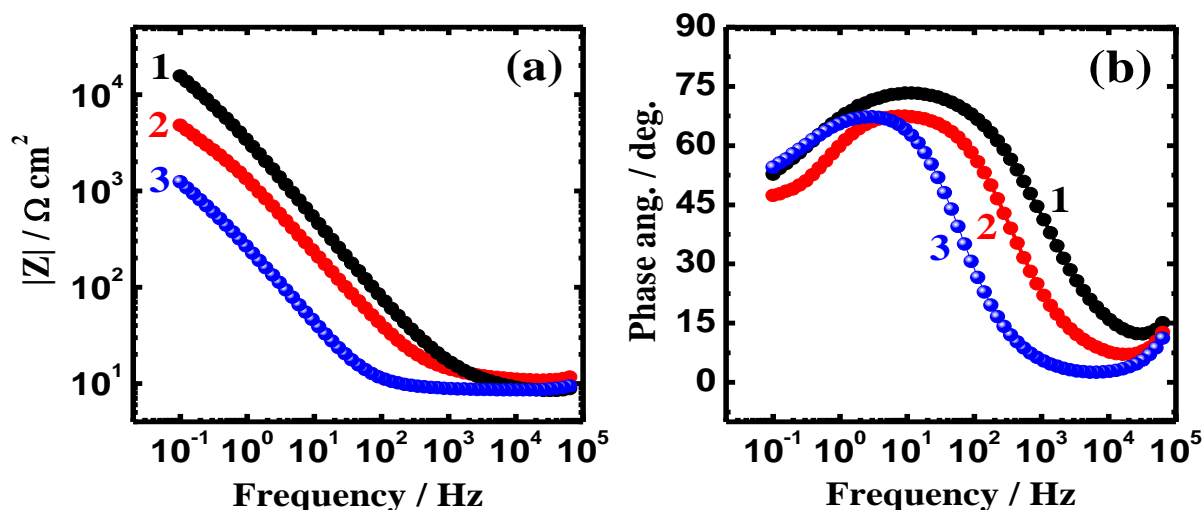

Figure 9. Bode (a) impedance of the interface and (b) phase angle plots obtained after 24 h immersion in 4% NaCl solutions for (1) pure Al, (2) Al-7%Cu, and (3) Al-7%Cu-3%Ti.

3.4. Chronoamperometric current-time measurements

Potentiostatic current-time curves obtained for (1) pure Al, (2) Al-7%Cu, and (3) Al-7%Cu-3%Ti electrodes, respectively after (a) 1.0 h and (b) 24 h immersion in 4.0% NaCl solutions before stepping the potential to -0.6 V vs. Ag/AgCl are shown in Figure 10. The current increased for the pure aluminum that was immersed for only 1.0 h (Figure 10a, curve 1) from the first moment of measurement to record almost 4.2mA/cm^2 then slightly decreased with time to record about 1.7mA/cm^2 after 1.0 h of applying the constant potential.

The presence of Cu as well as Ti decreased the initial current values but the currents were always increasing with time indicating that the pitting corrosion occurs at this condition for Al-7%Cu and Al-7%Cu-3%Ti alloys. The corrosion as well as the absolute current values at the end of the experiment were higher in the following order Al-7%Cu-3%Ti > Al-7%Cu > Al. The higher the absolute current values the higher the uniform corrosion, while the continuous increase of its value is due to the occurrence of pitting corrosion. Prolonging the immersion time to 24 h (Figure 10b) showed almost similar curves with similar behavior to those obtained after 1.0 h but with lower current values. This is because the increase of immersion time allows the aluminum and its alloys to form a layer of oxide or corrosion product on the surface, which decreases the chloride ions attack when applying the active potential value, -0.6 V vs. Ag/AgCl. In this regard, the uniform corrosion decreased but the pits

become wide and deeper as a result of the high attack of the chloride to the most weak and flawed areas on the surface.
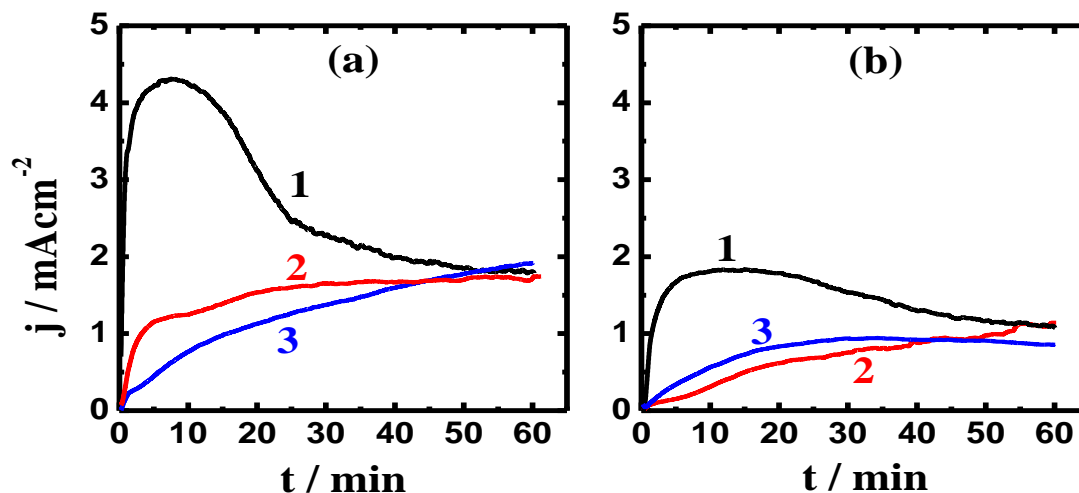

Figure 10. Potentiostatic current-time curves obtained for (1) pure Al, (2) Al-7%Cu, and (3) Al-7%Cu-3%Ti electrodes, respectively after (a) 1.0 h and (b) 24 h immersion in 4.0% NaCl solutions before stepping the potential to -0.6 V vs. Ag/AgCl.

3.5. Scanning electron microscope and energy dispersive X-ray investigations

In order to investigate the morphology as well as the chemical compositions of the surface of the obtained Al, Al-7%Cu and Al-7%Cu-3%Ti samples produced after 5.0 h ball mill time and after being immersed for 24 h in the chloride solutions, SEM and EDX investigations were carried out. Figure 11 shows (a) and (b) the SEM micrographs; (a') and (b') the EDX profile analyses taken from the surface of Al-7%Cu and Al-7%Cu-3%Ti, respectively after the two alloys were immersed for 24 h in 4.0% NaCl solutions before stepping the potential to -0.6 V vs. Ag/AgCl for 1.0 h. It is seen from the SEM image (Figure 11a) that the surface of the Al-Cu alloy is fully covered with thin corrosion product layer and there is a wide and deep pit. The EDX profile analysis depicted in Figure 11a' confirms that the corrosion products are aluminum oxide, aluminum chloride. This because the weight percentages of the elements obtained from the EDX profile were 80.63% Al, 4.53% Cu, 9.43% O, 2.37% C, 1.84% Cl, and 1.21% Na.

On the other hand, the SEM image obtained for the Al-Cu-Ti alloy (Figure 11b) shows a complete coverage for the surface with thick layer of corrosion products accompanied by small pits; most of these pits are probably covered with the corrosion products layer. The EDX profile analysis obtained from this surface and seen by Figure 11b' indicated that the weight percentages of the elements found were 72.70% Al, 7.50% Cu, 2.09% Ti, 12.00% O, 4.01% C, 1.00% Cl, and 0.69% Na. This indicates that the aluminum is selectively dissolves due to the harsh attack of the chloride ions under the most active anodic potential, -0.6 V vs. Ag/AgCl. Also, the corrosion products are mostly aluminum oxide and aluminum chloride. Moreover, the thick layer of the corrosion products covers the real surface of the alloy, which is why the percentage of Ti was lower than its normal percentage in the

alloy before corrosion testing. The SEM/EDX investigations thus confirm that the uniform as well as the pitting corroison occur for the two alloys and explain the increase of current with time as we have already seen from Figure 10b.
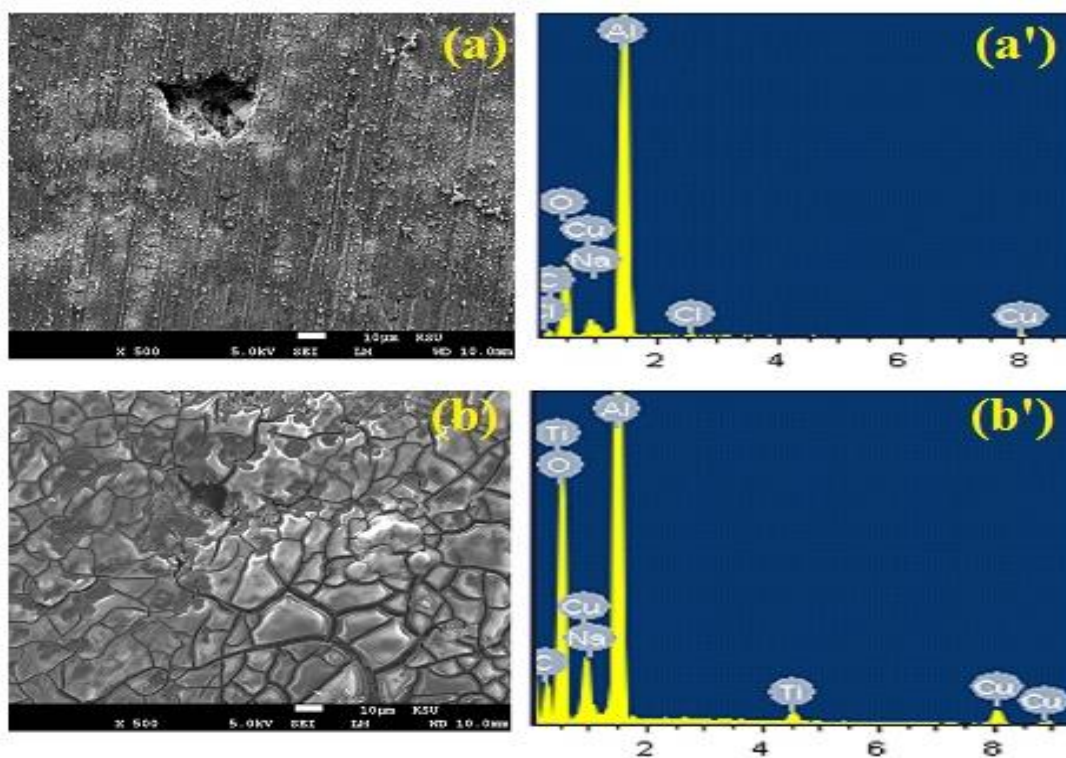

Figure 11. (a) and **(b)** are the SEM micrographs; while **(b)** and **(b')** are the EDX profile analyses taken from the surface of Al-7%Cu and Al-7%Cu-3%Ti, respectively after these alloys were immersed for 24 h in 4.0% NaCl solutions before stepping the potential to -0.6 V vs. Ag/AgCl for 1.0 h.

4. CONCLUSIONS

Manufacturing of nanocrystalline Al, nanocrystalline Al-7%Cu alloy and nanocrystalline Al-7%Cu-3%Ti alloy was carried out. All fabricated materials were characterized using XRD, Vickers hardness, SEM, and EDX investigations. The corrosion behavior after 1.0 h and 24 h immersion in 4.0% NaCl solutions was reported. The Vickers hardness was found to strongly increase in the presence of copper and titanium. Several techniques such as CPP, EIS, CCT, and SEM were employed to report the corrosion of Al, Al-7%Cu, and Al-7%Cu-3%Ti in the chloride test solution. CPP measurements indicated that the corrosion parameters like j_{Corr} and R_{Corr} increased, while the corrosion resistance decreased by the addition of Cu and further by the presence of Cu with Ti into Al. The EIS data also confirmed that the highest surface and polarization resistances were the highest for the pure aluminum. Further confirmation was also obtained from the current-time curves and SEM/EDX analysis where, all samples suffered both uniform corrosion and pitting corrosion. The severity of uniform corrosion increases in the order Al-7%Cu-3%Ti > Al-7%Cu > Al, while the pitting attack was decreasing the opposite order.

References

1. T. Choh, T. Oki, *Mater. Sci. Technol.*, 3 (1987) 378-385.
2. L. Ceschini, I. Boromei, G. Minak, A. Morri, F. Tarterini, *Compos. Sci. Technol.*, 67 (2007) 605-615.
3. M.L. Ted Guo, C.Y.A. Tsao, *Compos. Sci. Technol.*, 60 (2000) 65–74.
4. J.M. Torralba, F. Velasco, C.E. Costa, I. Vergara, D. Cáceres, *Composites Part A*, 33 (2002) 427-434.
5. M. Gupta, T.S. Srivatsan, *Mater. Lett.*, 51 (2001) 255-261.
6. C.M. Friend, *J. Mater. Sci.*, 22 (1987) 3005-3010.
7. T.G. Durai, K. Das, S. Das, *Mater. Sci. Eng. A*, 445-446 (2007) 100-105.
8. K. Kok, *Composites Part A*, 37 (2006) 457-464.
9. B. Bostan, A.T. Özdemir, A. Kalkanli, *Powder Metall.*, 47 (2004) 37-42.
10. A. Dolata-Grosz, J. Sleziona, B. Formanek, *J. Mater. Proc. Technol.*, 175 (2006) 192-197.
11. J.B. Fogagnolo, M.H. Robert, J.M. Torralba, *Mater. Sci. Eng. A*, 426 (2006) 85-94.
12. Z. Razavi Hesabi, A. Simchi, S.M. Seyed Reihani, *Mater. Sci. Eng. A*, 428 (2006) 159-168.
13. S. Goussous, W. Xu, X. Wu, K. Xia, *Compos. Sci. Technol.*, 69 (2009) 1997-2001.
14. El-Sayed M. Sherif, E.A. El-Danaf, M.S. Soliman, A.A. Almajid, *Int. J. Electrochem. Sci.*, 7 (2012) 2846-2859.
15. K. Shimizu, K. Kobayashi, V. Skeldon, G.E. Thompson, G.C. Wood, *Corros. Sci.*, 39 (1997) 701-718.
16. S.-m. Li, H.-r. Zhang, J.-h. Liu, *Trans. Nonferrous Metals Soc. China*, 17 (2007) 318-325.
17. C.M. Abreu, M.J. Cristóbal, R. Figueroa, G. Pena, *Corros. Sci.*, 54 (2012) 143-152.
18. J.D. Bessone, *Corros. Sci.*, 48 (2006) 4243-4256.
19. I. Gurrappa, *J. Mater. Proc. Technol.*, 166 (2005) 256-267.
20. C.F. Shrieber, J.I. Reding, *Mater. Prot.*, 6 (1967) 33-36.
21. T. Sakano, K. Toda, M. Hanada, *Mater. Prot.*, 5 (1996) 45-50.
22. S.M.A. Shibli, V.S. Gireesh, *Appl. Surf. Sci.*, 219 (2003) 203-210.
23. S.M.A. Shibli, S.R. Archana, A.P. Muhammed, *Corros. Sci.*, 50 (2008) 2232-2238 .
24. El-Sayed M. Sherif, J.A. Mohammed, H.S. Abdo, A.A. Almajid, *Int. J. Electrochem. Sci.*, 11 (2016) 1355-1369.
25. El-Sayed M. Sherif, H.R. Ammar, K.A. Khalil, *Appl. Surf. Sci.*, 301 (2014) 142-148.
26. R.S. Rana, Rajesh Purohit, S. Das, Int. J. Sci. Res. Publ., 2 (2012) 1-7.
27. S.G. Shabestari, H. Moemeni, J. Mater. Proc. Technol., 153–154 (2004) 193–198.
28. El-Sayed M. Sherif, H.S. Abdo, K.A. Khalil, A.M. Nabawy, *Metals*, 5 (2015) 1799-1811.
29. El-Sayed M. Sherif, *J. Ind. Eng. Chem.*, 19 (2013) 1884-1889.
30. H.F. Latief, El-Sayed M. Sherif, A.A. Almajid, H. Junaedi, *J. Anal. Appl. Pyrolysis*, 92 (2011) 485-492.